

# Direct simulation of turbulent flow in a pipe with annular cross-section

Maurizio Quadrio & Paolo Luchini

Dipartimento di Ingegneria Aerospaziale del Politecnico di Milano

via La Masa 34 - 20156 Milano

maurizio.quadrio@polimi.it

## Why the annular pipe?

- Incomplete experimental information (additional measuring difficulties in near-wall region) regarding turbulence statistics: see for example Nouri, Humur & Whitelaw, JFM 1993 **253**
- Effect of transverse curvature on turbulence not fully documented

## Objectives

- Numerical solution of incompressible NS equation (DNS) in annular geometry
- Extend to cylindrical coordinates a numerical method for the DNS of turbulent plane channel flow (adapt a computer code without structural changes)
- Perform DNS of the turbulent flow in an annular pipe (never reported)

## DNS of turbulence in cylindrical coordinates

- Numerical difficulties of cylindrical coordinate system → few DNS of turbulent flow in cylindrical geometries
- Most of the numerical schemes solve NS eqs in primitive variables, with the pressure-correction approach
- Only one DNS study (Neves, Moin & Moser, JFM 1994 **272**) considers transverse curvature, but is concerned with the boundary layer over small cylinders: approximate model problem, no outer wall, insufficient resolution in the outer layer

### The (standard) cartesian case

For plane channel flow, there is an almost standard procedure developed by Kim, Moin & Moser JFM 1987 **177**, by which:

- Pressure is eliminated from the equations
- NS system is reduced to a second-order scalar equation for the normal vorticity and a fourth-order scalar equation for the normal velocity
- When using Fourier transforms in homogeneous directions, the other velocity components are easily recovered
- High (nearly optimal) computational efficiency can be achieved

$$\frac{\partial u}{\partial x} + \frac{\partial v}{\partial y} + \frac{\partial w}{\partial z} = 0$$

$$\frac{\partial u}{\partial t} + H_u = -\frac{\partial p}{\partial x} + \frac{1}{Re} \nabla^2 u$$

$$\frac{\partial v}{\partial t} + H_v = -\frac{\partial p}{\partial y} + \frac{1}{Re} \nabla^2 v$$

$$\frac{\partial w}{\partial t} + H_w = -\frac{\partial p}{\partial z} + \frac{1}{Re} \nabla^2 w$$

### Cartesian case (cont.)

By applying  $\nabla \times$  to the momentum equation,  $\nabla \times \nabla p = 0$ . Considering the  $y$  component, one obtains for  $\omega_y = \partial u / \partial z - \partial w / \partial x$ :

$$\frac{\partial}{\partial t} \omega_y = \frac{1}{Re} \nabla^2 \omega_y + \frac{\partial H_u}{\partial z} - \frac{\partial H_w}{\partial x}$$

By manipulating momentum equation, and using continuity, one obtains for  $v$ :

$$\frac{\partial}{\partial t} \nabla^2 v = \frac{1}{Re} \nabla^4 v + \left( \frac{\partial^2}{\partial x^2} + \frac{\partial^2}{\partial z^2} \right) H_v - \frac{\partial}{\partial y} \left( \frac{\partial}{\partial x} H_u + \frac{\partial}{\partial z} H_w \right)$$

Initial conditions. Periodicity in  $x$  and  $z$ . No-slip boundary conditions at the walls:

$$v(x, z, \pm\delta) = 0; \quad v_y(x, z, \pm\delta) = 0; \quad \omega_y(x, z, \pm\delta) = 0$$

### Cartesian case (cont.)

- By Fourier transforming in the homogeneous directions,  $\hat{u}$  and  $\hat{w}$  are easily recovered with the solution of a **2x2 algebraic** system:

$$\begin{cases} \hat{u} = \frac{-i}{\alpha^2 + \beta^2} \left( \alpha \frac{\partial \hat{v}}{\partial y} - \beta \hat{w}_y \right) \\ \hat{w} = \frac{-i}{\alpha^2 + \beta^2} \left( \beta \frac{\partial \hat{v}}{\partial y} + \alpha \hat{w}_y \right) \end{cases}$$

- Implicit time schemes are usually **not** used, due to the need of accuracy over a wide range of spatial scales
- Partially implicit approach is very popular: **explicit** schemes for the **convective part**, but **implicit** schemes for the **viscous** terms (with time-scales smaller than those needing accurate representation)

### Cylindrical case

$$\frac{\partial u}{\partial x} + \frac{1}{r} \frac{\partial (rv)}{\partial r} + \frac{1}{r} \frac{\partial w}{\partial \theta} = 0$$

$$\frac{\partial u}{\partial t} + u \frac{\partial u}{\partial x} + v \frac{\partial u}{\partial r} + \frac{w}{r} \frac{\partial u}{\partial \theta} = - \frac{\partial p}{\partial x} + \frac{1}{Re} \nabla^2 u$$

$$\frac{\partial v}{\partial t} + u \frac{\partial v}{\partial x} + v \frac{\partial v}{\partial r} + \frac{w}{r} \frac{\partial v}{\partial \theta} - \frac{w^2}{r} = - \frac{\partial p}{\partial r} + \frac{1}{Re} \left( \nabla^2 v - \frac{v}{r^2} - \frac{2}{r^2} \frac{\partial w}{\partial \theta} \right)$$

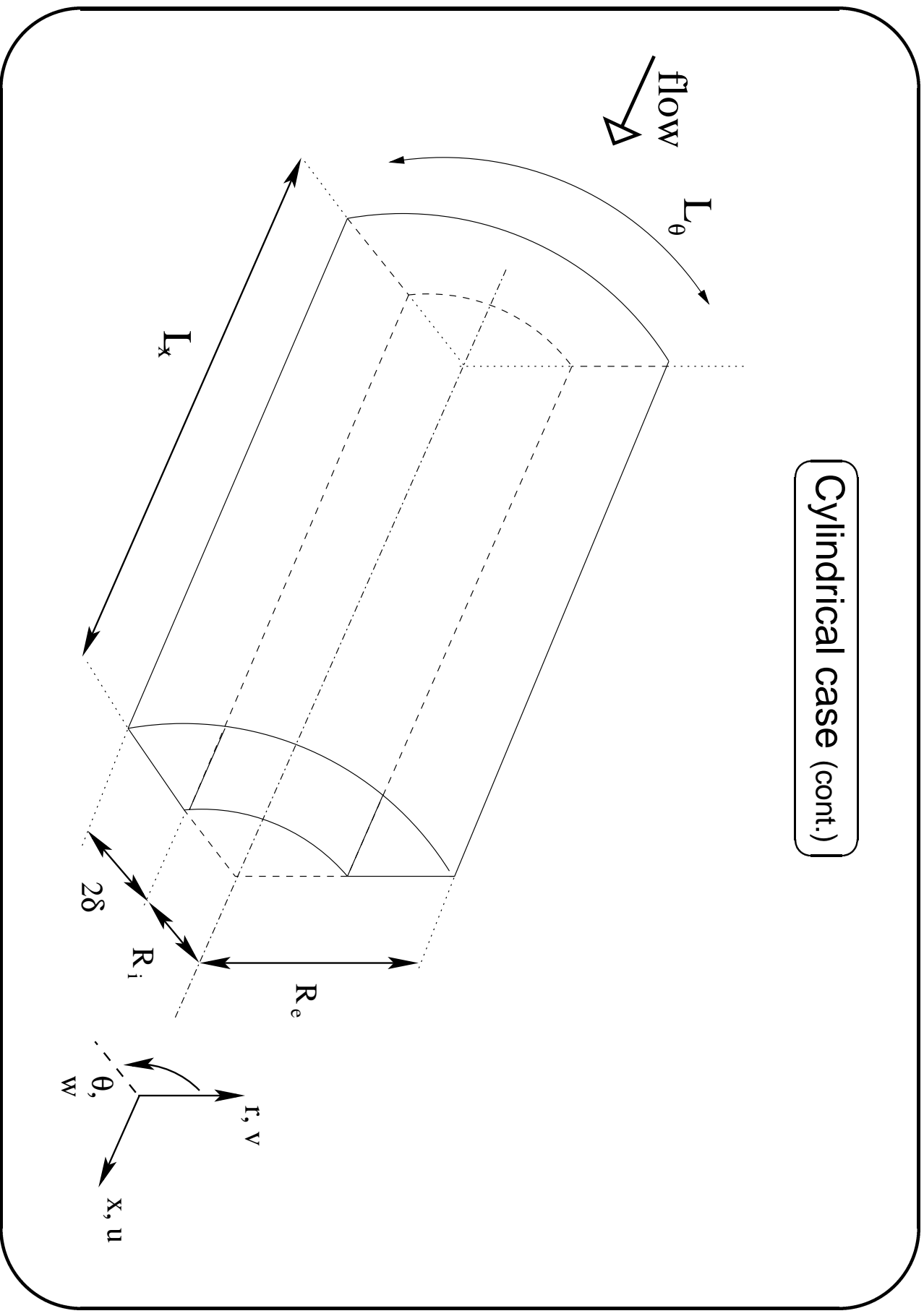
$$\frac{\partial w}{\partial t} + u \frac{\partial w}{\partial x} + v \frac{\partial w}{\partial r} + \frac{w}{r} \frac{\partial w}{\partial \theta} + \frac{vw}{r} = - \frac{1}{r} \frac{\partial p}{\partial \theta} + \frac{1}{Re} \left( \nabla^2 w - \frac{w}{r^2} + \frac{2}{r^2} \frac{\partial v}{\partial \theta} \right)$$

where

$$\nabla^2 = \frac{\partial^2}{\partial x^2} + \frac{1}{r} \frac{\partial}{\partial r} \left( r \frac{\partial}{\partial r} \right) + \frac{1}{r^2} \frac{\partial^2}{\partial \theta^2}$$



Cylindrical case (cont.)



### Cylindrical case (cont.)

By Fourier transforming the equations in homogeneous directions  $x$  (wave number  $\alpha$ ) and  $\theta$  (wave number  $m$ ) these difficulties are left:

- impossible implicit treatment of viscous terms: components of the momentum equation are coupled
- $k^2 = \alpha^2 + m^2/r^2$  depends on  $r$ !

Notation:

$$Df = \frac{\partial f}{\partial r}; \quad D_*f = \frac{\partial f}{\partial r} + \frac{f}{r} \quad \Rightarrow \quad \nabla^2 = -k^2 + D_*D$$

### The method: equation for $\omega_r$

In analogy with the cartesian case, by taking  $\nabla \times$  of the momentum equation and considering the  $r$  component, one obtains for radial vorticity  $\eta$ :

$$\frac{\partial \hat{\eta}}{\partial t} = \frac{1}{Re} \left( \nabla^2 \hat{\eta} - \frac{\hat{\eta}}{r^2} + 2 \frac{im}{r^2} D \hat{u} + 2 \frac{m\alpha}{r^2} \hat{v} \right) + \frac{im}{r} \hat{H}_u - i\alpha \hat{H}_w$$

- Not independent of  $\hat{v}$  anymore (no problem if equation for  $\hat{v}$  does not contain  $\hat{\eta}$ !)
- Contains two curvature terms  $\sim D \hat{u}$  and  $\hat{v}$
- Both  $\hat{v}$  and  $\hat{u}$  terms can enter the explicit part: low-order derivatives, presumably small since difference with cartesian, hence no stability problems

### The method: equation for $v$

- Continuity equation is Fourier transformed and time differenced
- Expressions for  $\partial \hat{u} / \partial t$  and  $\partial \hat{w} / \partial t$  are taken from momentum eq.
- Further simplifications by using continuity
- Solve for  $\hat{p}$ , then put  $D\hat{p}$  in  $r$  component of momentum eq.

$$\begin{aligned} \frac{\partial}{\partial t} \left[ \hat{v} - D \left( \frac{1}{k^2} D_* \hat{v} \right) \right] &= \\ &= \frac{1}{Re} D \left\{ \frac{1}{k^2} \left[ k^2 D_* \hat{v} - D_* D D_* \hat{v} - \frac{2m^2}{r^3} \hat{v} + 2 \frac{im}{r^2} D \hat{w} - 2 \frac{im}{r^3} \hat{w} \right] \right\} + \\ &+ \frac{1}{Re} \left( -k^2 \hat{v} + D D_* \hat{v} - 2 \frac{im}{r^2} \hat{w} \right) + D \left[ \frac{1}{k^2} \left( i\alpha \hat{H}_u + \frac{im}{r} \hat{H}_w \right) \right] + \hat{H}_v \end{aligned}$$

### The method: equation for $v$ (cont.)

- Independent of  $\hat{\eta}$
- Contains curvature terms  $\sim \hat{w}$
- Curvature terms can enter the explicit part, without stability problems

In analogy with the cartesian case,  $\hat{u}$  e  $\hat{w}$  are recovered with the solution of a 2x2 algebraic system:

$$\begin{cases} \hat{u} = \frac{1}{k^2} \left( i\alpha D_* \hat{v} - \frac{im}{r} \hat{\eta} \right) \\ \hat{w} = \frac{1}{k^2} \left( i\alpha \hat{\eta} + \frac{im}{r} D_* \hat{v} \right) \end{cases}$$

As in cartesian case, for  $k^2 = 0$  the  $x$  and  $\theta$  components of the momentum equation are to be solved directly.

## The numerical solution

- FFT algorithms allow exact computation of the nonlinear terms in physical space; De-aliasing with the 3/2 rule.
- Radial derivatives discretized with finite differences over a 5-point stencil; low-order derivatives are IV order, higher order derivatives are II<sup>nd</sup> order → formally II<sup>nd</sup> order method, but advantageous compared to a II<sup>nd</sup> order scheme
- Time integration: as in KMM, third-order Runge-Kutta for the explicit part, and second-order Crank-Nicholson for the implicit part.

## The physical problem

- Periodicity assumption in  $x$  and  $\theta$  directions
- Inner radius  $\mathcal{R}_i$ , outer radius  $\mathcal{R}_o$ ; gap  $\mathcal{R}_o - \mathcal{R}_i = 2\delta$
- Constant flow rate; after reaching steady state, computations are carried out for  $150 tU_b/\delta$ , storing flow fields every  $15 tU_b/\delta$
- $Re = U_b\delta/\nu = 2800$ , where  $U_b$  is bulk velocity; corresponds to  $\mathcal{R}_i^+ \sim 185$  (case 1) and  $\mathcal{R}_i^+ \sim 370$  (case 2)
- $\alpha_0 = 0.5$  which gives  $L_x = 4\pi\delta$ 
  - case 1:  $m_0 = 1$  which gives  $2\pi\delta \leq L_\theta \leq 6\pi\delta$
  - case 2:  $m_0 = 2$  which gives  $2\pi\delta \leq L_\theta \leq 4\pi\delta$

## Transversal resolution & cylindrical coordinates

- For a given  $m_0$ , transversal size of the computational domain increases with  $r$
- Physical considerations dictate resolution needed at outer wall
- Resolution increases (linearly) above necessary approaching inner wall  
⇒ waste of computational resources, and potential stability problems
- With Fourier schemes, Fourier series must be truncated at wavenumber corresponding to maximum resolution

## Solution

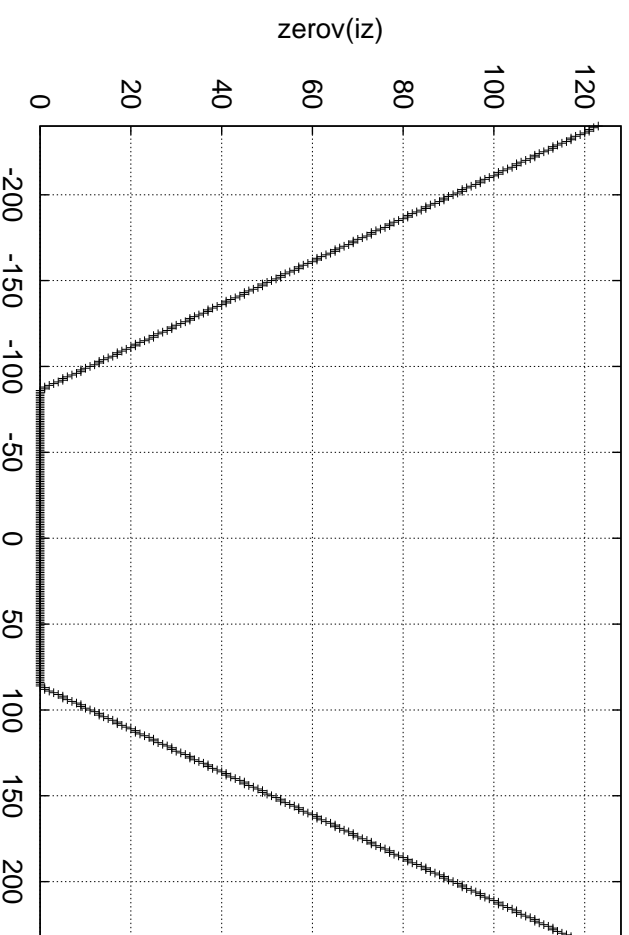
An  $r$ -dependent truncation of the series can remove unneeded azimuthal modes, saving memory and CPU time, and avoiding stability problems.



### Transversal resolution (cont.)

Azimuthal resolution variable with coordinate  $r$  is implemented thanks to a suitable memory management.  
Linear  $r$ -dependency.

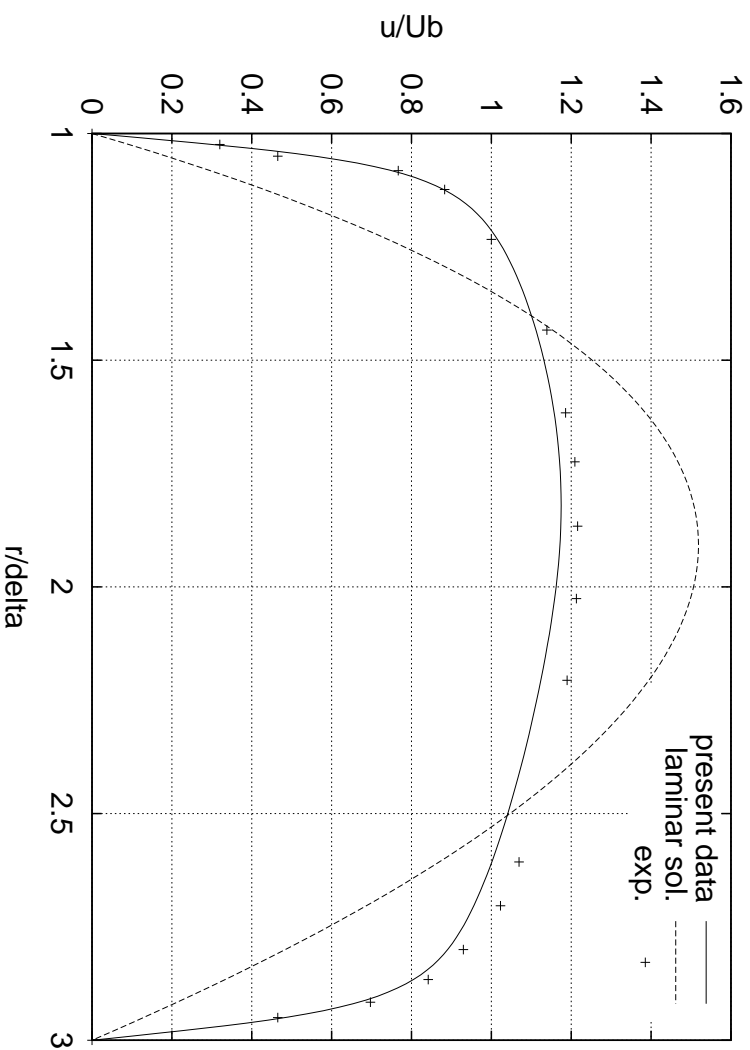
2d array of pointers into a variable-sized 1d array



## Computational parameters (case 2 only)

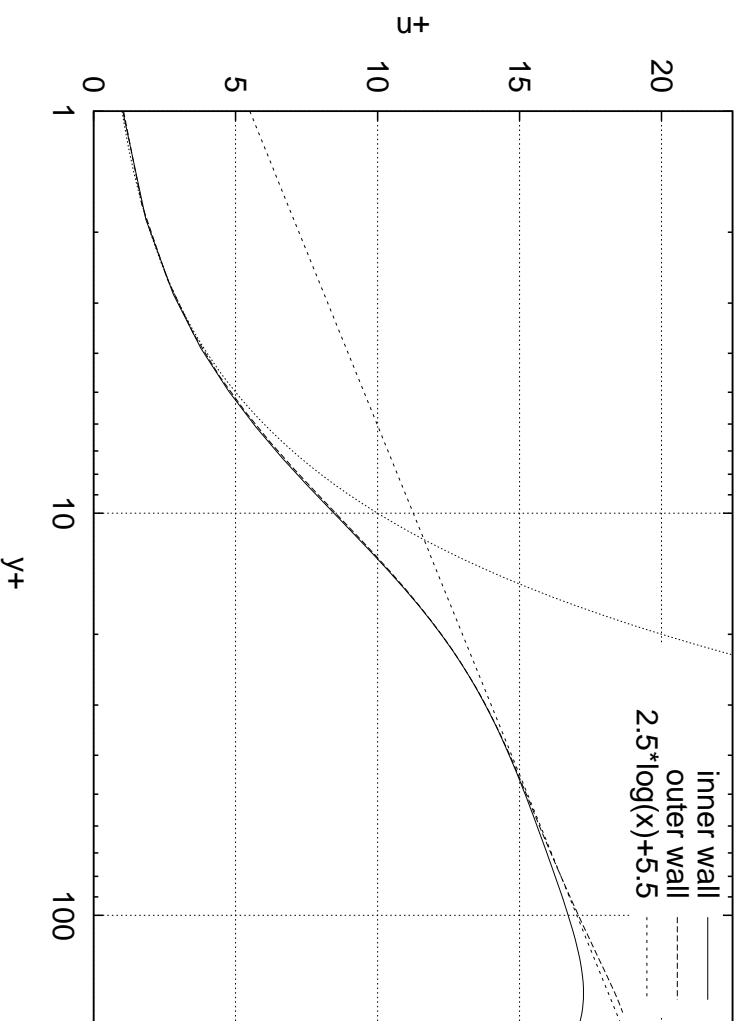
- Radial range divided in 128 (uneven) intervals
- 193 Fourier modes in axial direction:  $-96 \leq \alpha/\alpha_0 \leq +96$
- 481 Fourier modes in  $\theta$  direction at  $r = \mathcal{R}_o$ :  $-240 \leq m/m_0 \leq +240$ ; they linearly reduce to 161 at  $r = \mathcal{R}_i$
- Spatial resolution is very high:  $\Delta x^+ \sim 11.7$ ;  $\Delta z^+ \sim 7$ ;  $\Delta r^+ = 0.9 - 4.5$
- 16 millions d.o.f.; RAM memory: 410MB; single flow field on disk: 136MB
- 250 seconds / time step for a SMP personal computer (2 CPU Intel 550MHz); parallel speedup of 100%
- Time step  $0.02 tU_b/\delta$  (comparable to planar case); computing time  $\sim 3$  weeks

## Mean velocity profile, $\mathcal{R}_i^+ = 185$



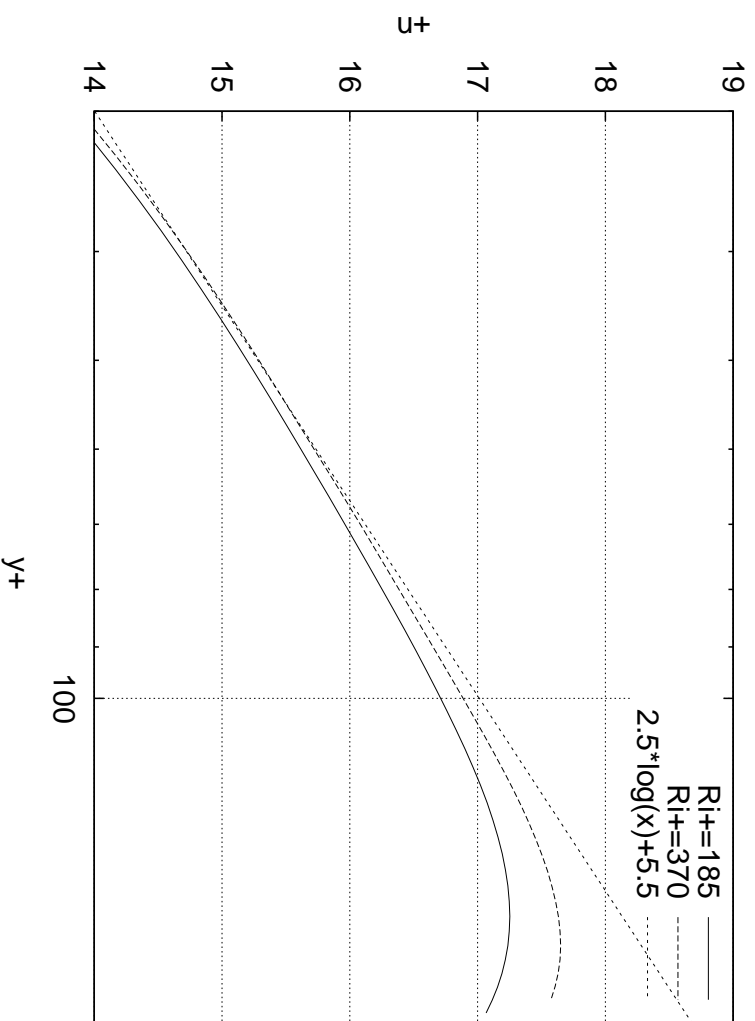
Curvature causes asymmetry: velocity maximum towards the inner wall, higher friction on the inner side.

## Law of the wall



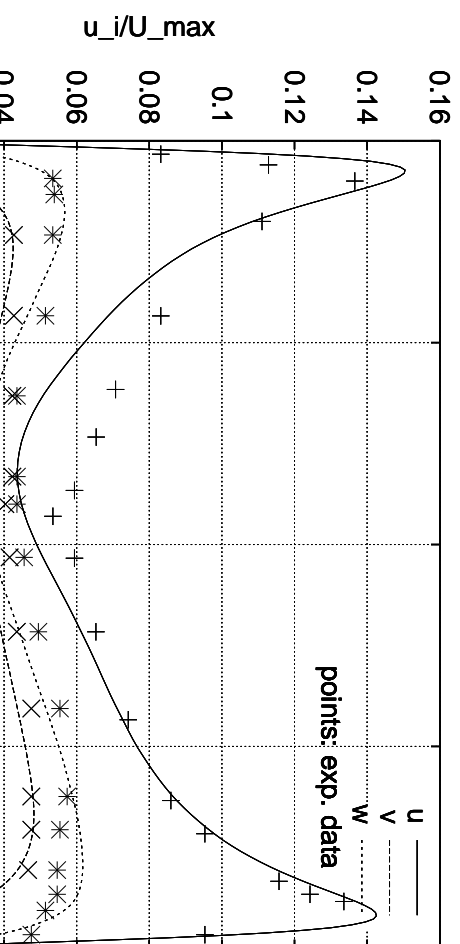
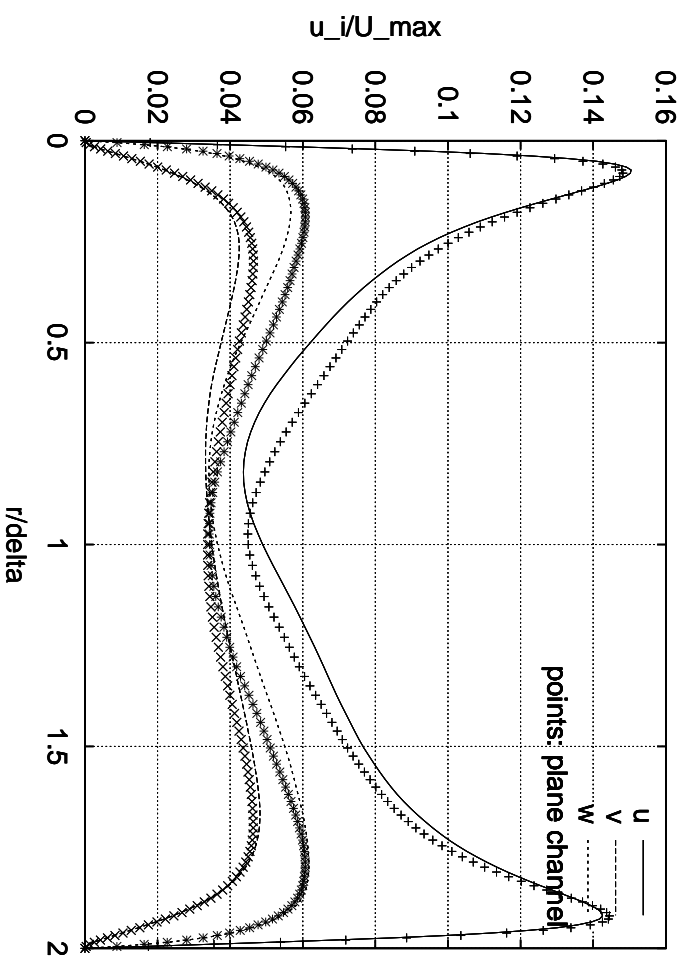
- Velocity profile follows standard log law over the external wall, with some effects in the outer region
- Effects of curvature on the inner wall, down to

### Law of the wall (cont.)



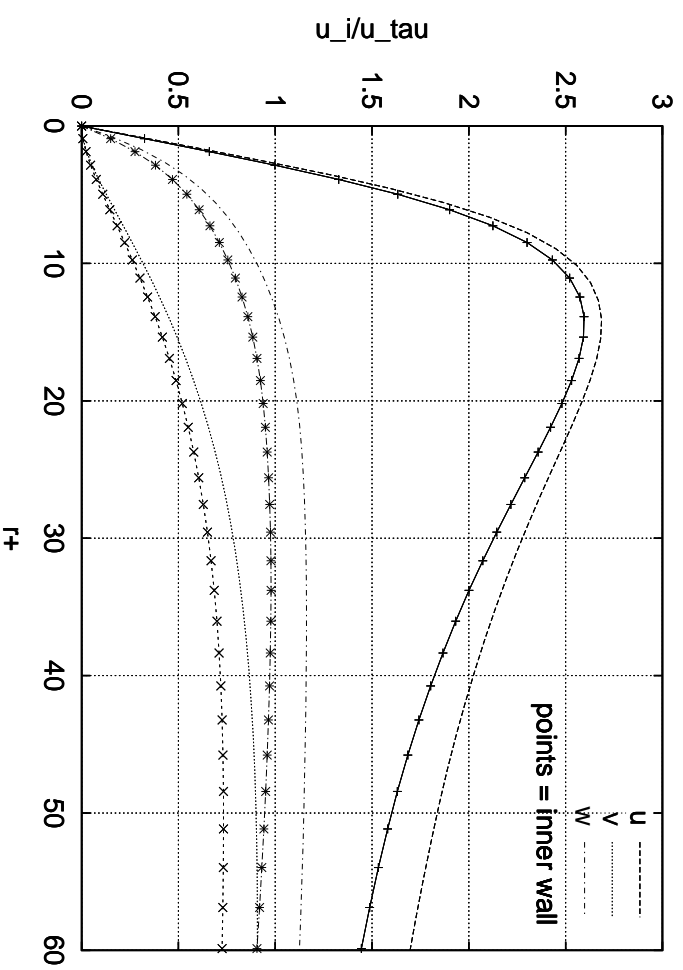
- Decreasing slope in the log region with increasing curvature
- Careful parametric study needed for assessing

# RMS velocity fluctuations



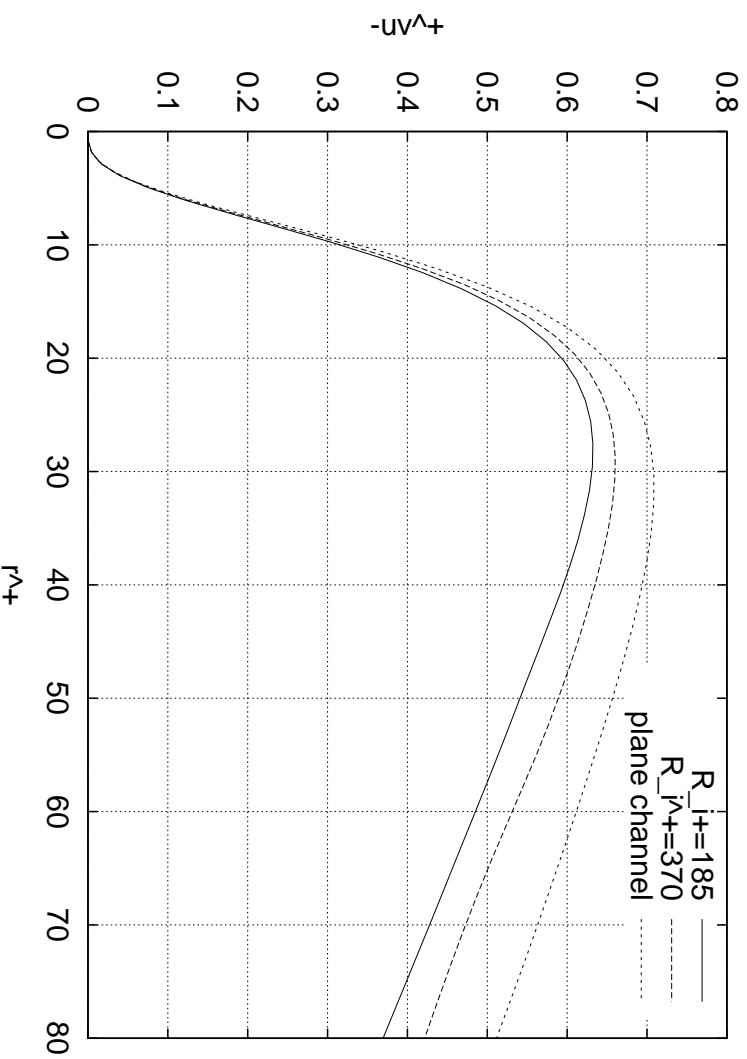
### RMS velocity fluctuations (cont.)

Normalization with friction velocity



- Curvature causes reduction of turbulence intensities.
- Maximum effect on radial and azimuthal components.

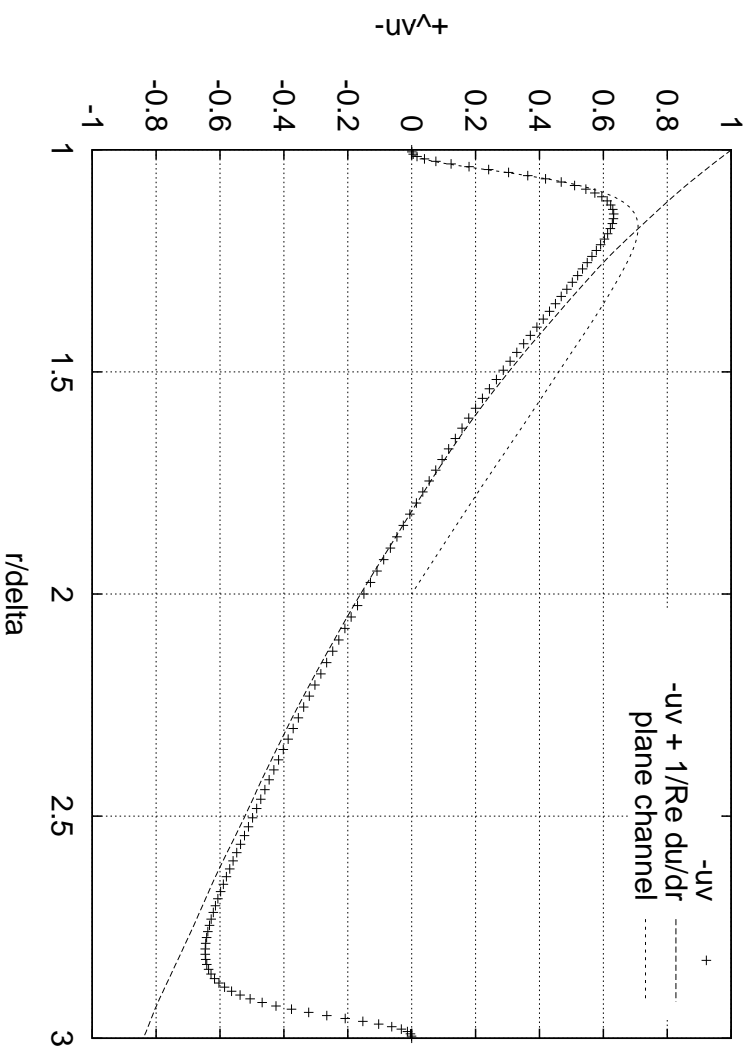
## Turbulent stresses



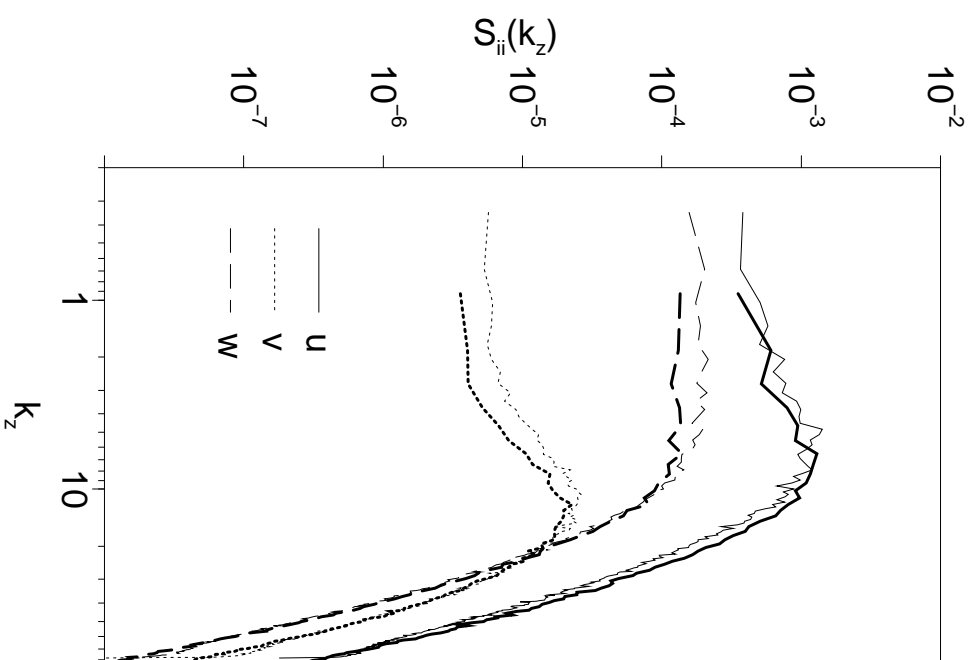
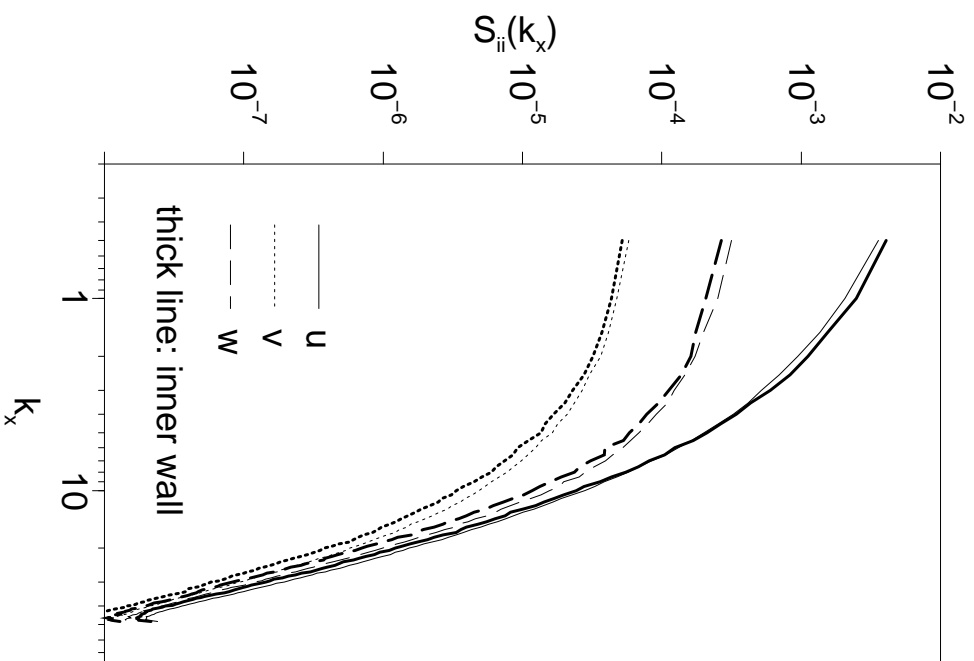
- The effect of curvature is to reduce the Reynolds shear stress.
- The point of maximum moves towards the wall with



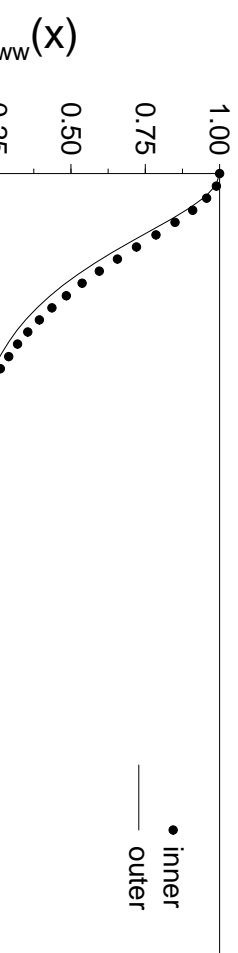
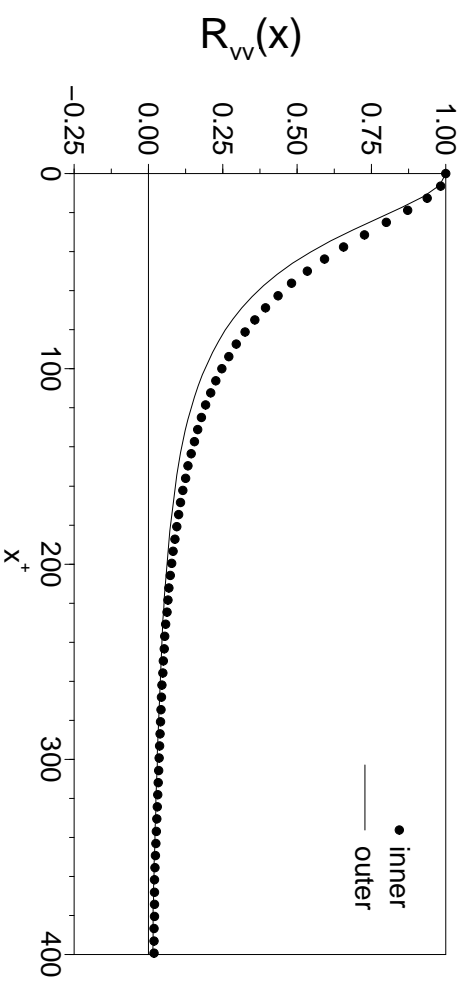
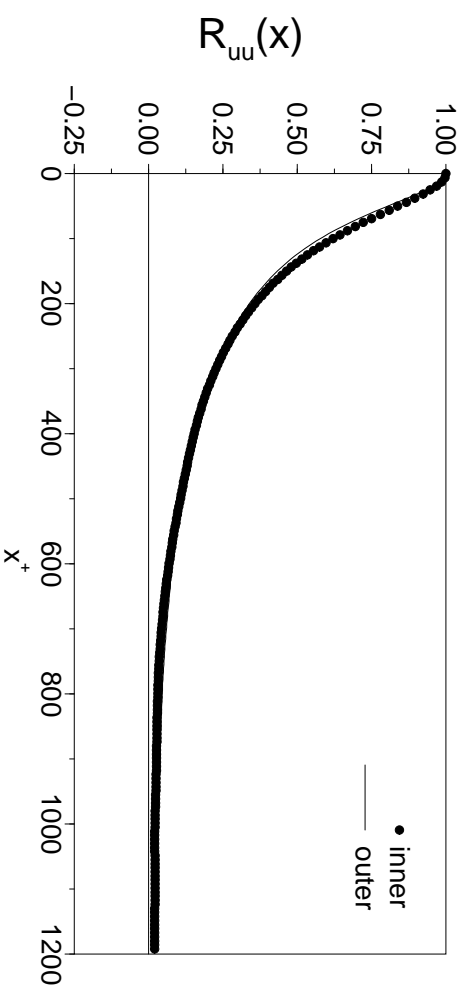
### Turbulent stresses (cont.)



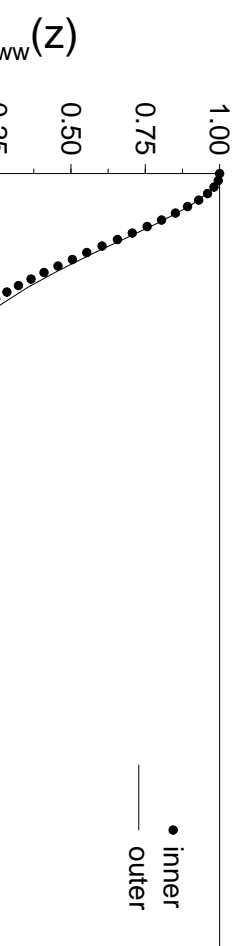
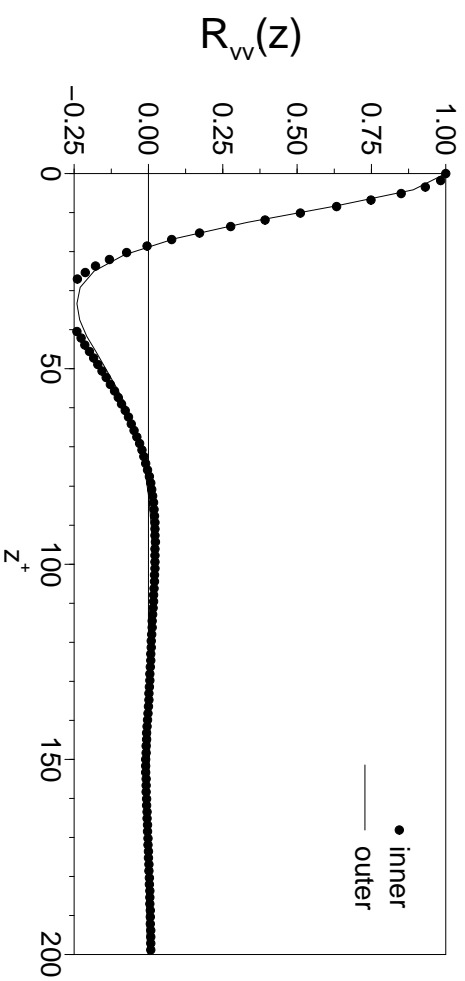
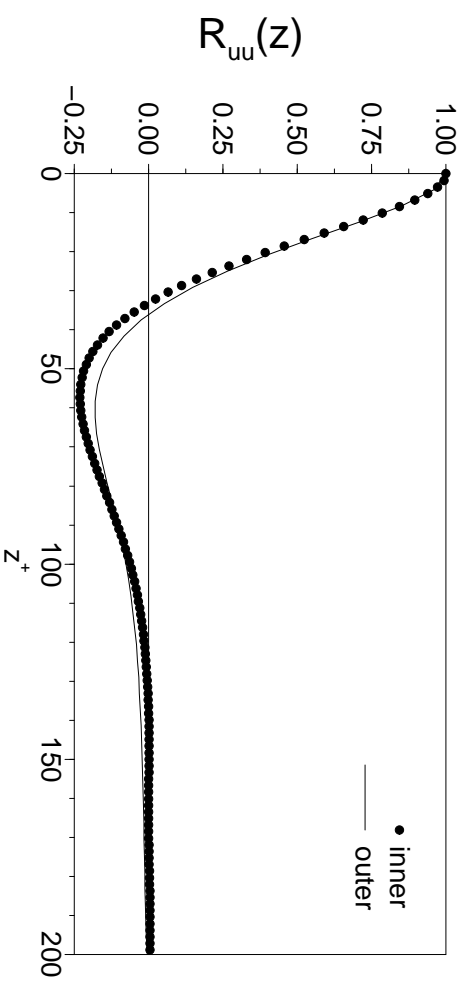
- Integration time enough for reaching the statistical steady state

**1-d energy spectra,  $r^+ = 15$** 

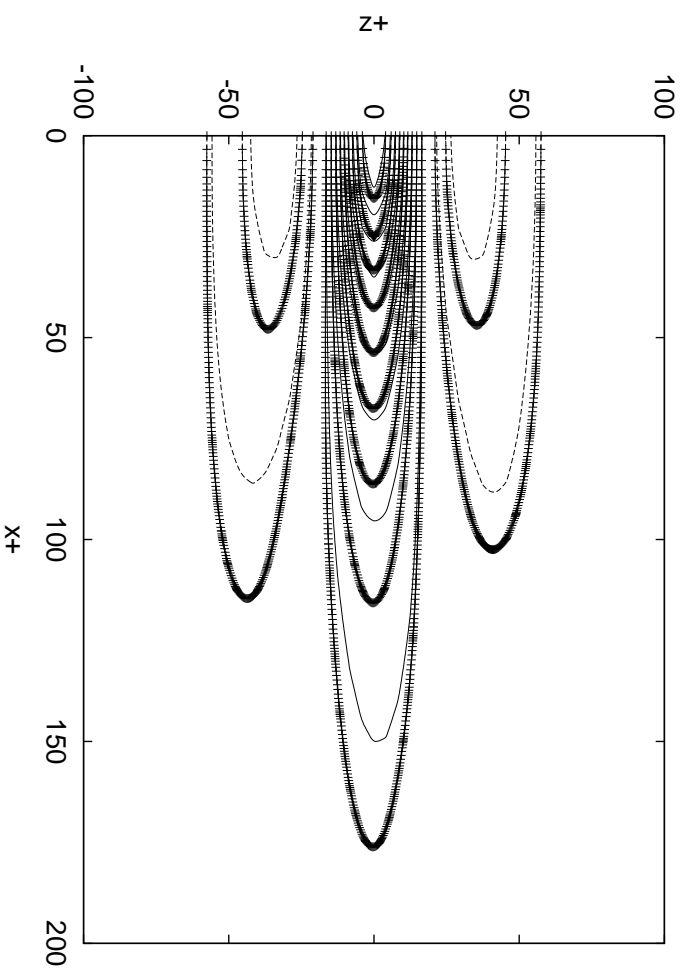
## Axial correlations



## Azimuthal correlations

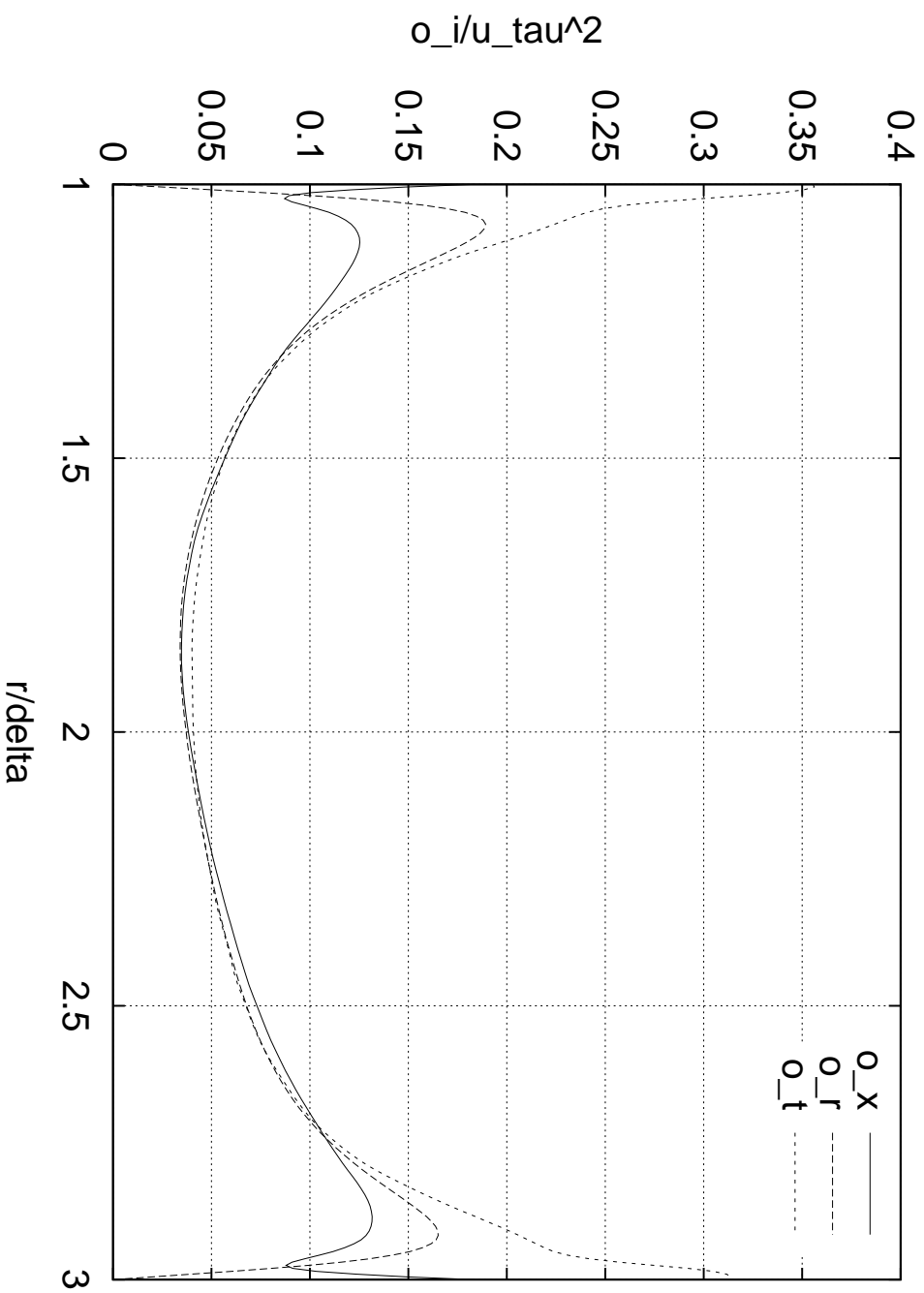


## Plane autocorrelation, $v$ component

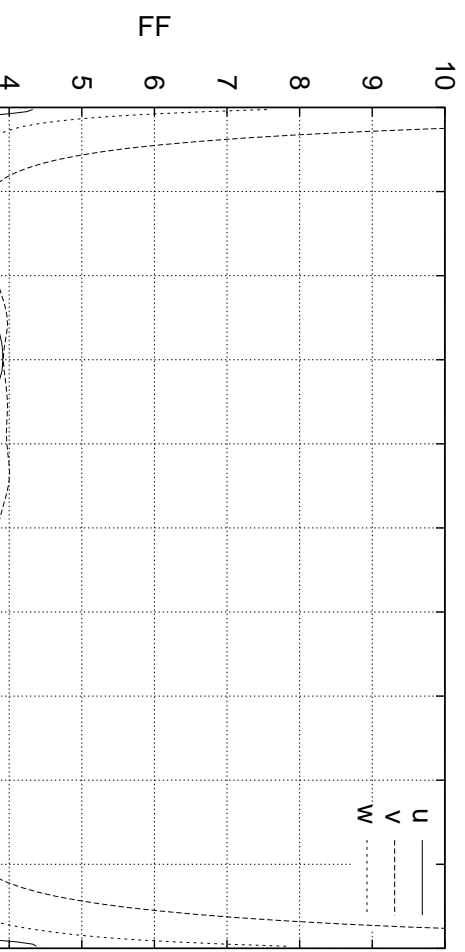
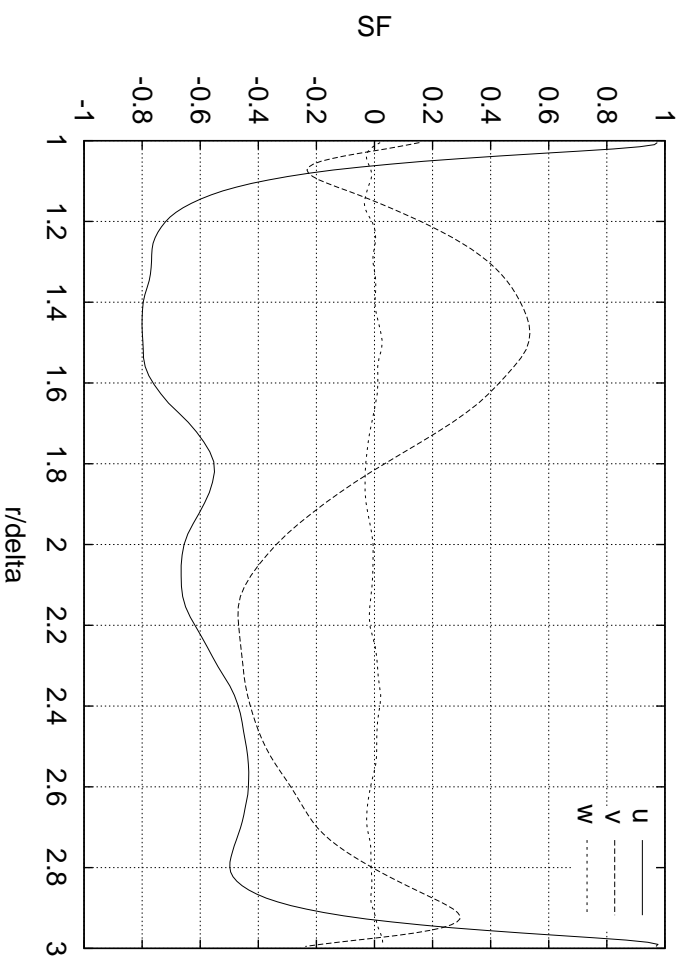


- Symbols: inner wall. Solid lines: positive values. Increment 0.1
- Correlation length increases with curvature

## RMS vorticity fluctuations



## Skewness and flatness factor



## Conclusions

- An efficient method for DNS of turbulent flows in cylindrical geometries has been presented, as an extension of the cartesian case
- The number of Fourier modes in  $\theta$  direction has been varied with  $r$ , so that the azimuthal resolution is constant: significant benefits
- Turbulent flow in the annular pipe has been studied for the first time via DNS
- Preliminary observations on the effect of the transverse curvature on the turbulence statistics have been reported